

Modelling of Hg adsorption on activated carbon in WtE plant fabric filters

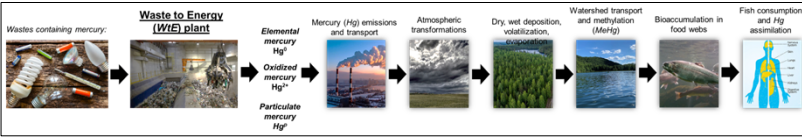
Senem Ozgen^a, Simone Speroni^{a,b}, Antonio Conversano^b

^a LEAP s.c.a.r.l. – Laboratorio Energia e Ambiente Piacenza, Via Nino Bixio 27/C, 29121, Piacenza (PC), Italy

^b Dipartimento di Energia, Politecnico di Milano, P.zza Leonardo da Vinci 32, 20133 Milano (MI), Italy

Corresponding author: senem.ozgen@polimi.it

MERCURY PROBLEM



AIMS OF THE STUDY

Development of a model using a kinetic approach to describe the mercury adsorption process on activated carbon based on data from a full-scale solid waste incineration plant equipped with a dry flue gas treatment line. Previous literature on mercury removal with activated carbon was studied and critical points in modelling to go beyond the state-of-the-art were identified and implemented in the present study.

MERCURY ADSORPTION ON ACTIVATED CARBON IN A FABRIC FILTER

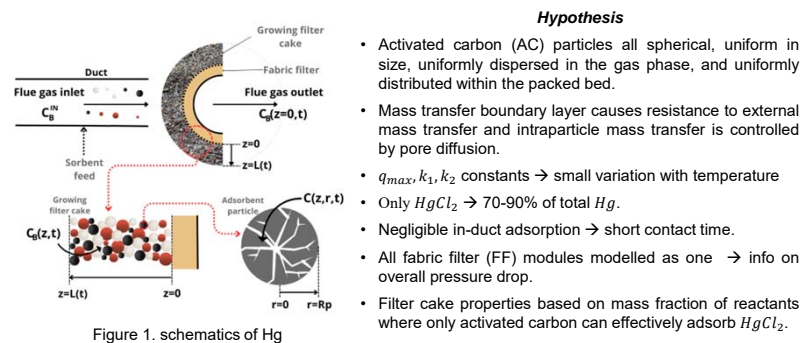


Figure 1. schematics of Hg

Hypothesis

- Activated carbon (AC) particles all spherical, uniform in size, uniformly dispersed in the gas phase, and uniformly distributed within the packed bed.
- Mass transfer boundary layer causes resistance to external mass transfer and intraparticle mass transfer is controlled by pore diffusion.
- q_{max}, k_1, k_2 constants \rightarrow small variation with temperature
- Only $HgCl_2 \rightarrow 70-90\%$ of total Hg.
- Negligible in-duct adsorption \rightarrow short contact time.
- All fabric filter (FF) modules modelled as one \rightarrow info on overall pressure drop.
- Filter cake properties based on mass fraction of reactants where only activated carbon can effectively adsorb $HgCl_2$.

MODELLING

The model is based on the pore diffusion mechanism and Langmuir theory for the equilibrium between the gas phase and the surface of activated carbon particles. It neglects in-duct adsorption and focuses on Hg adsorption solely within the growing bed deposited on the fabric filter surface.

Adsorption on activated carbon
$$\frac{\partial q}{\partial t} = k_{1,m}(q_{max,m} - q)C - k_{2,m}q$$

Intraparticle mass transfer
$$\epsilon_{b,tot} \frac{\partial C_B}{\partial t} = u \frac{\partial C_B}{\partial z} - \frac{3\rho_{b,tot} D_e}{\rho_{p,m} R_{p,m}} \frac{Q_{AC1} + Q_{AC2}}{\rho_{b,AC1} + \rho_{b,AC2}} \frac{\partial C}{\partial r} \Big|_{(z,R_p,t)}$$

External mass transfer
$$\epsilon_{p,m} \frac{\partial C}{\partial t} = D_e \left(\frac{\partial^2 C}{\partial r^2} + \frac{2}{r} \frac{\partial C}{\partial r} \right) - \rho_{p,m} [k_{1,m}(q_{max,m} - q)C - k_{2,m}q]$$

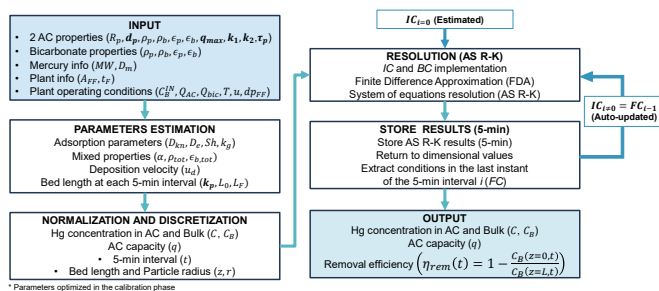
Initial conditions
IC $\begin{cases} q(z,r,t_i=0) = q(z,r,t_{i-1} = t_F) \\ C(z,r,t_i=0) = C(z,r,t_{i-1} = t_F) \\ C_B(z,r,t_i=0) = C_B(z,r,t_{i-1} = t_F) \\ L(t_i=0) = L_0 \end{cases}$

Boundary conditions
BC $\begin{cases} C_B(z=L,t) = C_B^N \\ q(z=L,r,t) = 0 \\ C(z=L,r,t) = 0 \\ \frac{\partial C_B}{\partial z} \Big|_{(z=0,t)} = 0 \\ \frac{\partial C}{\partial r} \Big|_{(z,r=R_p,t)} = \frac{k_g}{D_e} [C_B(z,t) - C(z,R_p,t)] \\ \frac{\partial q}{\partial r} \Big|_{(z,r=0,t)} = 0 \\ \frac{\partial C}{\partial r} \Big|_{(z,r=0,t)} = 0 \end{cases}$

$C = HgCl_2$ concentration in the gas phase of the internal pore (kg of $HgCl_2/m^3$)
 $C_B = HgCl_2$ concentration in the bulk gas phase of the filter cake (kg of $HgCl_2/m^3$)
 $D_e =$ effective pore diffusion coefficient (m^2/s)
 $k_1 =$ Adsorption rate constant ($m^3 kg^{-1} s^{-1}$)
 $k_2 =$ Desorption rate constant (s^{-1})
 $k_g =$ Gas-phase mass-transfer coefficient (m/s)
 $k_p =$ bed constant (m/mbar s)
 $L =$ Filter cake thickness (m)
 $Q_{AC} =$ Sorbent loading in the flue gas (kg/m^2)
 $Q_{bic} =$ Bicarbonate loading in the flue gas (kg/m^2)
 $q =$ Hg adsorbed on the sorbent (kg/kg_{AC})
 $q_{max} =$ maximum adsorption capacity (kg_{Hg}/kg_{AC})
 $R_{p,m} =$ Radius of the particle (m)
 $r =$ Sorbent radial distance (m)
 $u =$ superficial gas velocity (m/s)
 $\epsilon_b =$ bed porosity (-)
 $\epsilon_p =$ particle porosity (-)
 $\rho_b =$ bed density (kg/m^3)
 $\rho_p =$ sorbent particle density (kg/m^3)
 $d_p =$ pore diameter (μ)
 $\tau_p =$ tortuosity factor
 $m =$ mixed properties
 $tot =$ total

MODEL IMPLEMENTATION

The coordinate transformation technique and finite difference approximation was applied to make the system of differential equations (i.e., Langmuir equation, Hg mass balance along the bed and inside the AC particle) more tractable and solvable with an adaptive step size Runge-Kutta solver. With respect to previous studies which considered static operating conditions, the model developed in the present study takes into consideration the Hg concentration variability at the FF inlet and the simultaneous injection of two different types of activated carbon



MODELLING APPROACH REFERENCES

- Scala, F. (2001). Environmental Science and Technology, 35(21), 4373–4378.
- Flora, J. R. V., et al., 2003. Journal of the Air and Waste Management Association, 53(4), 478–488.
- Scala, F. (2004). Industrial and Engineering Chemistry Research, 43(10), 2575–2589.
- Li, X., Lee, J. Y. (2013). Energy and Fuels, 27(12), 7654–7663.

RESULTS

- The model has undergone calibration and subsequent validation using datasets particularly chosen including high and low Hg concentrations (19'500 five-minute average data points)
- When employing consistent Langmuir constants (i.e., q_{max}, k_1, k_2) across different inlet Hg concentrations, the calculated Hg removal efficiency seemed to be underestimated, particularly for low Hg inlet concentrations (below $20 \mu g/m^3$).

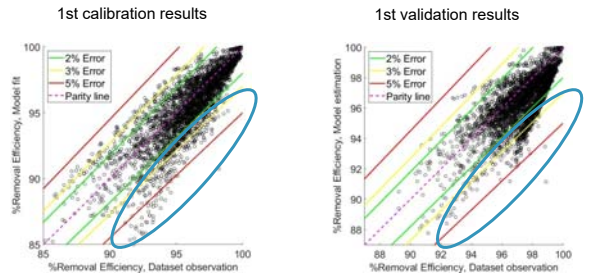


Figure 2. First calibration and validation results: for Hg inlet concentration under $20 \mu g/Nm^3$ (blue curve) the model tends to underestimate the removal efficiency.

- As a result, the model was recalibrated independently for inlet Hg concentrations above and below the abovementioned threshold. The outcome notably improved.
- Overall, the model demonstrated the capability to estimate Hg removal efficiency in the FF unit with a maximum absolute error margin of $\pm 3\%$ and a mean absolute percentage error of 0.87%.

Table 1. Calibration parameters, optimal ranges and optimized values for the fabric filter mercury adsorption model

Calibration parameter	Optimization range	1 st optimized value	2 nd optimized value	
$q_{max,AC1}$ (kg/kg)	$10^{-5} - 5 \cdot 10^{-1}$	$4.88 \cdot 10^{-1}$	$<20 \mu g/m^3$	$>20 \mu g/m^3$
$k_{1,AC1}$ ($m^3/kg \cdot s$)	$10^1 - 5 \cdot 10^3$	10 ²	$4.95 \cdot 10^{-1}$	$4.81 \cdot 10^{-1}$
$k_{2,AC1}$ (s^{-1})	$10^0 - 10^{-1}$	$3.63 \cdot 10^{-3}$	$1.04 \cdot 10^2$	$1.08 \cdot 10^2$
$q_{max,AC2}$ (kg/kg)	$10^{-5} - 5 \cdot 10^{-1}$	$6.09 \cdot 10^{-2}$	$2.85 \cdot 10^{-3}$	$5.17 \cdot 10^{-2}$
$k_{1,AC2}$ ($m^3/kg \cdot s$)	$10^1 - 5 \cdot 10^3$	$1.01 \cdot 10^3$		$1.11 \cdot 10^3$
$k_{2,AC2}$ (s^{-1})	$10^0 - 10^{-1}$	$5.44 \cdot 10^{-2}$		$5.48 \cdot 10^{-2}$
$d_{p,AC1}$ (m)	$5 \cdot 10^{-10} - 5 \cdot 10^{-8}$	$8.27 \cdot 10^{-9}$		$9.31 \cdot 10^{-9}$
$d_{p,AC2}$ (m)	$5 \cdot 10^{-10} - 5 \cdot 10^{-8}$	$2.05 \cdot 10^{-8}$		$2.03 \cdot 10^{-8}$
k_p (m/mbar s)	$10^0 - 10^5$	$9.64 \cdot 10^0$		$8.49 \cdot 10^0$
$\tau_{p,AC1}$	$5 \cdot 10^0 - 65 \cdot 10^1$	$5.00 \cdot 10^0$		$5.21 \cdot 10^0$
$\tau_{p,AC2}$	$5 \cdot 10^0 - 65 \cdot 10^1$	$8.16 \cdot 10^0$		$8.01 \cdot 10^0$
Mean absolute percentage error (MAPE)		1.32%	0.87%	

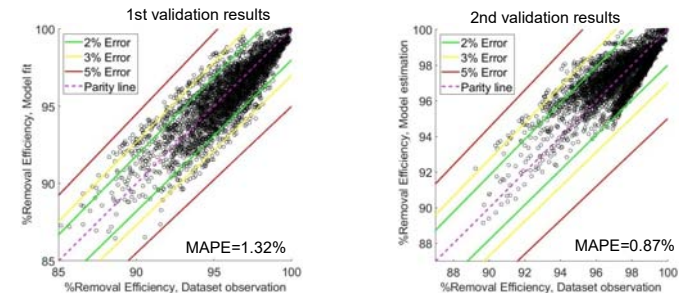


Figure 3. Validation comparison of the recalibrated model: (left panel: 1st model - 328 validation data points outside 3% error band; right panel: recalibrated model - only 59 data points outside 3% error band)

CONCLUSIONS

- The model performance indicators confirmed the effectiveness of the applied methodology but there is potential for further improvement.
- A critical review of the initial hypotheses could amplify the complexity of the phenomenon's description.
 - This could involve incorporating elemental mercury, currently overlooked, and accounting for the packing phenomenon in the filter cake.
- Additionally, investigating the delay between flue gas entry and exit from the FF presents another point for exploration.
- Further refinement of the model includes optimizing the algorithm employing more robust resolution techniques, enhancing the accuracy and minimizing the computation time.

FUTURE DEVELOPMENTS

- The model was developed with the intention of integrating it into phenomenological models for the creation of virtual sensors, specifically for mercury monitoring in Waste-to-Energy plants. These virtual sensors serve as backups in the event of stack mercury analyzer failures, bridging the monitoring gap until the physical analyzers are reinstated.
- The model has also the potential to play a key role in a data-driven activated carbon feed control strategy, thereby contributing to increased economic and environmental sustainability in WtE plants.

Related paper: Speroni et al., 2024. Mercury adsorption on activated carbon in Waste-to-Energy: model development and validation on real plant data. Waste Management 184:72-81.